Supplementary Information (SI) for

Predictions of moiré excitons in twisted two-dimensional organic-inorganic halide perovskites

Linghai Zhang[†], Xu Zhang[†], and Gang Lu[*,†]

[†]Department of Physics and Astronomy, California State University, Northridge, Northridge, California 91330-8268, United States

[*]Corresponding author. Email: ganglu@csun.edu

Computational Methods

First-principles ground state calculations

The ground state properties of MA_2PbI_4 homobilayers were calculated using Vienna Ab initio Simulation Package.[1] The Perdew-Burke-Ernzerhof (PBE) exchange-correlation functional[2] and projector-augmented wave pseudopotentials[3] with an energy cutoff of 400 eV were used in all the calculations. Empirical DFT-D2 correction[4] was employed to describe the van der Waals interaction. All the atomic structures were fully optimized until the residual force on each atom was less than 0.02 eV/Å. A vacuum spacing of ~15 Å in the out-of-plane direction was used to eliminate spurious interaction between the periodic images. The non-twisted MA_2PbI_4 bilayers were constructed by cleaving the cubic bulk $MAPbI_3$ along its (001) surface. To determine the atomic structure and single-particle band structure of the non-twisted MA_2PbI_4 bilayers, the Γ-centered $6 \times 6 \times 1$ and $8 \times 8 \times 1$ Monkhorst-Pack grids were used, respectively, to sample the Brillouin zones. The atomic structures of the twisted bilayers were generated by using CellMatch software.[5] The lattice mismatch in the twisted MA_2PbI_4 homobilayers of $\theta=11.3°$ and $\theta=8.1°$ was 0.94% and 0.48%, respectively. Only the Γ point was sampled in the Brillouin zone to obtain the optimized atomic structures of the twisted MA_2PbI_4 bilayers. The Γ-centered $2 \times 2 \times 1$ and $1 \times 1 \times 1$ Monkhorst−Pack grids were used to determine the single-particle band structures of the twisted MA_2PbI_4 bilayer with $\theta=11.3°$ and $\theta=8.1°$, respectively.

First-principles excited state calculations

The so-called GW-Bethe-Salpeter equation (GW-BSE) method[6-8] is the commonly used first-principles approach to capture excitonic effect in semiconductors. However, the GW-BSE approach is prohibitively expensive to deal with the moiré excitons owing to the large number of atoms (up to 2058 atoms) in the unit cell. To circumvent the problem, we have recently developed an alternative first-principles method that can provide a reliable description of excitonic effect with much less computational cost.[9-11] Our method is based on linear-response time-dependent density functional theory (LR-TDDFT)[12] with optimally tuned, screened and range-separated hybrid exchange-correlation functionals (OT-SRSH).[13-15] In this method, there are three parameters, α, β, and γ, needed to be specified. α determines the contribution from the short-range exact exchange and with β together

satisfies the expression: $\alpha + \beta = 1/\varepsilon_0$. The scalar dielectric constant (ε_0) of the MA_2PbI_4 bilayer was set to 7.6 in our calculations. The three parameters (α = 0.05, β =0.08, γ= 0.15) were obtained by fitting the fundamental bandgap of MA_2PbI_4 bilayer (in the A stacking) from DFT-OT-SRSH calculations to that from the PBE0 hybrid functional with the spin-orbit coupling (SOC) correction. The exciton binding energy is defined as the difference between the fundamental bandgap and the optical bandgap· Using the above parameters in (TD)DFT-OT-SRSH calculations, the exciton binding energy is estimated as 0.20 eV for the A stacking configuration, which is close to the value (0.17 eV) reported in bulk MA_2PbI_4.[16] Owing to the large unit cells (up to 2058 atoms), only the Γ-point was sampled in the Brillouin zone in TDDFT-OT-SRSH calculations. The (TD)DFT-OT-SRSH method has been used to study excitonic properties in a wide range of semiconductors, such as 2D halide perovskites, TMDs, conjugated organics and phosphorene.[11, 17-20] More details and validations of the (TD)DFT-OT-SRSH method can be found in these references.

Spin-orbit coupling (SOC) correction

Owing to the presence of the heavy element Pb in RP halide perovskites, SOC correction may be important for single-particle band structure calculations. To examine the SOC effect on the band structure, we used PBE+SOC to compute the single-particle band structure for the twisted MA_2PbI_4 bilayer with θ=11.3° and compare the results to those from PBE calculations without the SOC correction. As shown in Table S2 and Figure S6, while the SOC correction is significant on the CBM bandwidth, it is much smaller on the VBM bandwidth. The VBM bandwidth changes from 9 meV (PBE) to 11 meV (PBE+SOC) and the band compositions are the same with or without the SOC correction. Because CBM is contributed primarily by Pb, the SOC correction is significant. In contrast, VBM arises mainly from I, which is a lighter element, the SOC correction is much smaller. Hence, the SOC correction does not change the main conclusion in terms of the formation of flat valence bands in the twisted MA_2PbI_4 bilayers. Therefore, we did not include the SOC correction in our first-principles calculations owing to the high computational demand.

Table S1. The shortest H bond lengths (d_{TH} and d_{BH}), the vertical dipole moment (in Debye) and the binding energy (in meV/atom) in the primitive unit cells of the four stacking configurations. The binding energy (E_{bind}) of a bilayer material is defined by the following equation: $E_{bind} = (E_{bilayer} - 2\times E_{monolayer})/N$. Here $E_{bilayer}$, $E_{monolayer}$, and N represent the total energy of the bilayer, the monolayer, and the total number of atoms in the unit cell, respectively. A negative binding energy indicates that the bilayer is energetically more stable than the two separate monolayers.

stacking configuration	d_{TH} (Å)	d_{BH} (Å)	vertical dipole moment	binding energy
A	3.28	3.60	0.06	-12
B	5.45	5.73	0.08	-3
C	4.43	4.61	0.08	-6
D	4.21	5.00	0.41	-7

Table S2. The bandwidth of CBM and VBM (in meV) of the non-twisted (A stacking configuration) and the twisted MA_2PbI_4 bilayers.

	A stacking (PBE)	θ=11.3° (PBE)	θ=11.3° (PBE+SOC)	θ=8.1° (PBE)
CBM	1340	43	101	34
VBM	321	9	11	0

Table S3. The calculated fundamental bandgap (E_g), optical bandgap (E_{opt}), and exciton binding energy (E_b) of the twisted MA_2PbI_4 bilayers under different electric fields by using (TD)DFT-OT-SRSH method.

Electric field (V/nm)	θ=11.3° (eV)			θ=8.1° (eV)		
	E_g	E_{opt}	E_b	E_g	E_{opt}	E_b
0	2.64	2.48	0.16	2.59	2.48	0.11
-3	2.36	2.21	0.15	2.38	2.26	0.12
-5	2.27	2.12	0.15	2.23	2.12	0.11

	-6	2.19	2.04	0.15	2.15	2.03	0.12

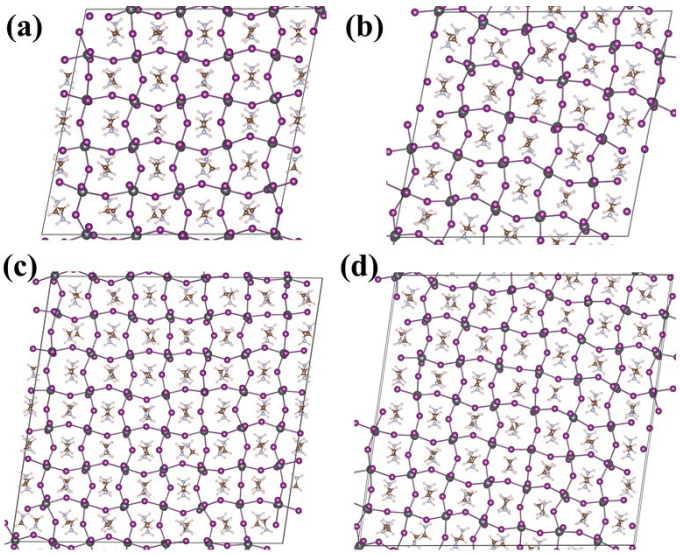

Figure S1. The top layer (a) and bottom layer (b) of the twisted MA_2PbI_4 bilayer with θ=11.3°. The top layer (c) and bottom layer (d) of the twisted MA_2PbI_4 bilayer with θ=8.1°.

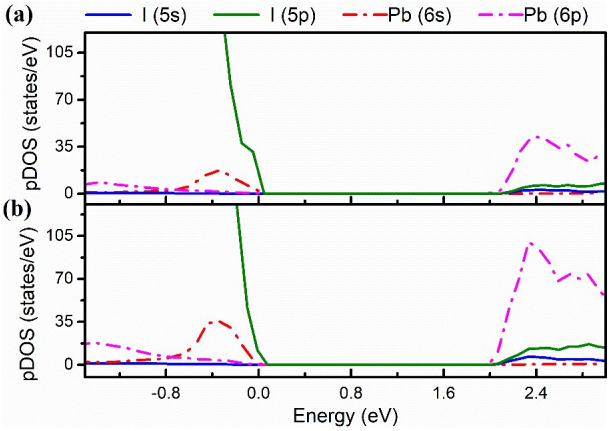

Figure S2. The projected density of states (pDOS) of the twisted MA_2PbI_4 bilayer with θ=11.3° (a) and θ=8.1° (b).

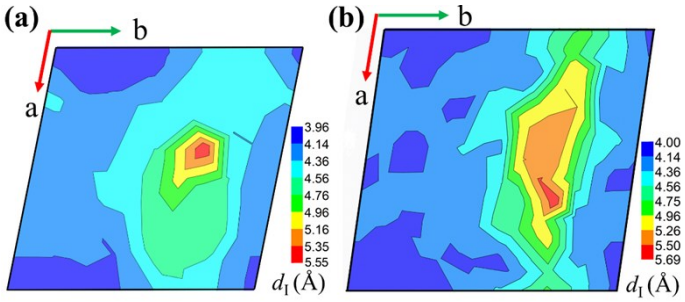

Figure S3. The shortest I-I distance (d_I) between the two layers in the twisted MA_2PbI_4 bilayer with θ=11.3° (a) and θ=8.1° (b).

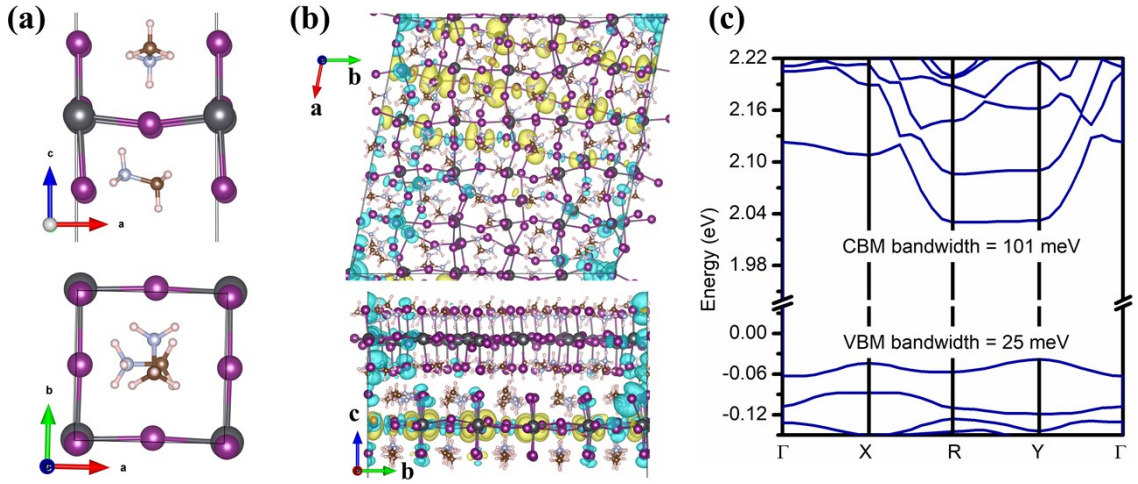

Figure S4. (a) The primitive unit cell of MA_2PbI_4 monolayer with a new orientation of MA cations (the MA cations in the monolayer are now perpendicular to each other). (b) The charge density of the lowest energy excitons of the twisted MA_2PbI_4 bilayer (θ=11.3°) with the new orientation of MA cations. The hole and electron densities (iso-surface value set at 0.0001 e/Å^3) are shown in cyan and yellow color, respectively. (c) The band structure of the twisted MA_2PbI_4 bilayer (θ=11.3°) with the new orientation of MA cations. The Fermi level is set to zero.

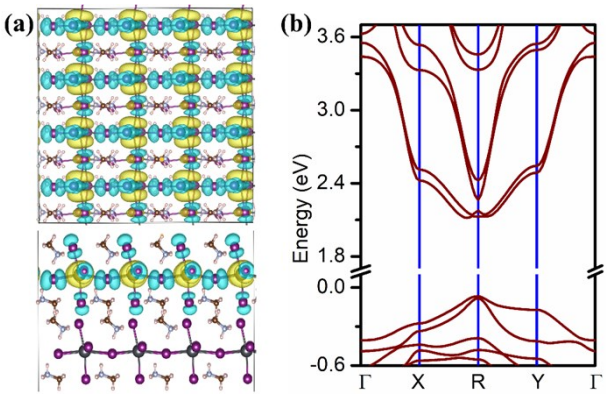

Figure S5. (a) The charge density of the lowest energy exciton in the non-twisted bilayer under the pressure. The hole and electron densities (iso-surface value set at 0.0001 e/Å^3) are shown in cyan and yellow color, respectively. (b) The single-particle band structure of the non-twisted bilayer under the pressure.

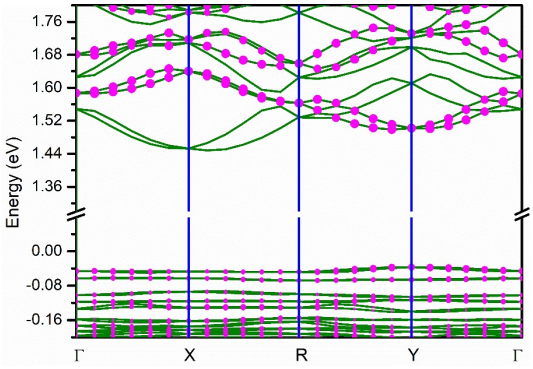

Figure S6. The single-particle band structure of the twisted MA_2PbI_4 bilayer with θ=11.3° using PBE+SOC. The Fermi level is set to zero. The relative contribution from the top layer is indicated by the size of pink dots in each band (the absence of the dots suggests no contribution from the top layer).

References

1. G. Kresse and J. Furthmüller, *Phys. Rev. B*, 1996, **54**, 11169-11186.
2. J. P. Perdew, K. Burke and M. Ernzerhof, *Phys. Rev. Lett.*, 1996, **77**, 3865–3868.
3. P. E. Blöchl, *Phys. Rev. B*, 1994, **50**, 17953-17979.
4. S. Grimme, *J. Comput. Chem.*, 2006, **27**, 1787-1799.

5. P. Lazić, *Comput. Phys. Commun.*, 2015, **197**, 324-334.
6. L. Hedin, *Phys. Rev.*, 1965, **139**, A796-A823.
7. M. S. Hybertsen and S. G. Louie, *Phys. Rev. B*, 1986, **34**, 5390-5413.
8. M. Rohlfing and S. G. Louie, *Phys. Rev. B* 2000, **62**, 4927-4944.
9. X. Zhang, Z. Li and G. Lu, *J. Phys. Conden. Matt.* , 2012, **24**, 205801.
10. L.-y. Huang, X. Zhang, M. Zhang and G. Lu, *J. Phys. Chem. C*, 2017, **121**, 12855-12862.
11. L.-y. Huang, X. Zhang, M. Zhang and G. Lu, *Phys. Rev. Materials*, 2018, **2**, 054003.
12. E. Runge and E. K. U. Gross, *Phys. Rev. Lett.*, 1984, **52**, 997-1000.
13. S. Refaely-Abramson, S. Sharifzadeh, M. Jain, R. Baer, J. B. Neaton and L. Kronik, *Phys. Rev. B*, 2013, **88**, 081204.
14. L. Kronik and J. B. Neaton, *Annu. Rev. Phys. Chem.*, 2016, **67**, 587-616.
15. S. Refaely-Abramson, M. Jain, S. Sharifzadeh, J. B. Neaton and L. Kronik, *Phys. Rev. B*, 2015, **92**, 081204.
16. X. Zhu, Z. Xu, S. Zuo, J. Feng, Z. Wang, X. Zhang, K. Zhao, J. Zhang, H. Liu, S. Priya, S. F. Liu and D. Yang, *Energy Environ. Sci.*, 2018, **11**, 3349-3357.
17. H. Guo, X. Zhang and G. Lu, *Sci. Adv.* , 2020, **6**, eabc5638.
18. J. Liu, X. Zhang and G. Lu, *Nano Lett.* , 2020, **20**, 4631-4637.
19. J. Liu, Z. Li, J. Wang, X. Zhang, X. Zhan and G. Lu, *J. Mater. Chem. A*, 2020, **8**, 23304-23312.
20. Y. Gao, M. Zhang, X. Zhang and G. Lu, *J. Phys. Chem. Lett.*, 2019, **10**, 3820-3827.